Fryer, P., Pearce, J. A., Stokking, L. B., et al., 1990
Proceedings of the Ocean Drilling Program, Initial Reports, Vol. 125

5. STRUCTURE OF THE OUTER IZU-BONIN FOREARC FROM SEISMIC-REFLECTION PROFILING AND GRAVITY MODELING[1]

Robert L. Horine,[2] Gregory F. Moore,[3] and Brian Taylor[3]

ABSTRACT

Geophysical surveys conducted over the trench and lower trench slope of the Izu-Bonin arc have provided new information on the timing and mode of formation of several seamounts in this region. Multichannel seismic data reveal that these seamounts contain a shallow cap (less than 1 km thick) without internal reflections, which dredging and coring results indicate is made of serpentinite. This cap is underlain by a seismically reflective region that may be the original substrate onto which the serpentinite protruded. Sedimentary sequences flanking the seamounts have been uplifted. Gravity data indicate that the forearc near the seamounts is composed of low-density material that extends as deep as the décollement. These seamounts have experienced several periods of deformation, with the seamount at 30°55'N, 141°47'E having undergone very recent, perhaps even current, uplift. A two-stage process is proposed for the formation of these seamounts. The first stage would consist of small serpentinite diapirs breaching the surface to form serpentinite volcanoes. In the second stage, uplift of the seamounts would result from serpentinite intrusions into the volcanoes and a widening zone of serpentinization around the feeder conduits.

INTRODUCTION

As part of a regional investigation conducted prior to Ocean Drilling Program (ODP) Leg 125 drilling, extensive geophysical surveys were made over the Izu-Bonin arc. These surveys include the 96-trace multichannel seismic-reflection (MCS) data collected using the *Fred H. Moore* of the University of Texas Institute for Geophysics. In this chapter, we present and interpret the MCS data as well as model marine gravity data collected in 1979 by the Geological Survey of Japan. Specifically, we examine the internal structures of several seamounts on the inner trench slope and the depositional pattern of the sediment flanking these features to develop a model for the timing and mode of formation of these seamounts.

The Izu-Bonin arc marks an intraoceanic convergent plate boundary where the Pacific Plate is being subducted beneath the Philippine Sea Plate. Many aspects of the subduction process are poorly understood, particularly those concerning coupling between the two plates within the first 150 km of the trench. Two end-member models have been proposed for the mechanical interaction in this region: accretion and tectonic erosion.

Tectonic erosion is a process whereby material is removed from the overriding plate and carried down into the mantle by the subducting slab. This process could result in subsidence of the forearc and will result in landward migration of the trench. Hussong and Uyeda (1982) and Bloomer (1983) proposed that this process was active in the Mariana arc. Tectonic erosion may also be occurring in the Izu-Bonin arc, as suggested by Crawford et al. (1981) and Sakai et al. (in press).

Accretion is essentially the opposite of erosion. During accretion, material from the subducting oceanic crust is scraped off and added to the forearc, resulting in seaward migration of the trench and some uplift of the forearc. In regions with a significant sediment influx, such as the Lesser Antilles (Westbrook and Smith, 1983) or Nankai (Aoki et al., 1982), large accretionary prisms have formed. However, there is little sediment in the Izu-Bonin Trench, so the Izu-Bonin arc has only a small accretionary wedge (Horine et al., 1988).

Accretion and erosion are mechanical interactions. Chemical interactions, such as those produced by dewatering of the subducting slab, are also possible. As the oceanic crust descends into a higher temperature and pressure regime, low-temperature hydrous minerals, such as clays, recrystallize to a more stable phase, such as amphibole, releasing excess water (Sakai et al., in press). The path that this water takes back to the surface, whether along the décollement or directly through the overriding slab, provides information about the mechanical nature of the forearc. The water will follow the path of least resistance, which would be fractures in a brittle forearc or the décollement in a ductile forearc. Chemical reactions between the water and the host rock may also create effects that are detectable at the surface, such as serpentinite diapirism. A series of seamounts on the landward slope of the Mariana Trench appears to be diapirs of this type (Fryer et al., 1984), and similar seamounts occur in the Izu-Bonin arc (Ishii et al., in press; Maekawa et al., in press).

The geophysical surveys over the lower slope of the Izu-Bonin arc were positioned to take advantage of features that facilitate study of the deep structure of the arc. The thin sedimentary cover permits resolution of many structures near the surface. The presence of inferred serpentinite diapirs in the forearc may result from processes deep within the arc.

GEOLOGIC BACKGROUND

The Izu-Bonin arc (Fig. 1) marks the northeast edge of the Philippine Sea. This arc is bounded to the north by Honshu, Japan, and to the south by the Mariana arc. The Izu-Bonin Trench is a roughly linear feature that reaches depths of over 9500 m and strikes approximately 350° (Honza and Tamaki, 1985). The Pacific Plate in this region is moving almost due west, so that the subduction beneath this arc has about 10° of obliquity. The subduction rate is 50 mm/yr at the southern end of the arc and 70 mm/yr at the northern end (Seno et al., 1987). This plate configuration appears to have been stable since the Miocene, when the opening of the Shikoku Basin to the west rotated the arc into its present position (Kodama et al., 1983;

[1] Fryer, P., Pearce, J. A., Stokking, L. B., et al., 1990. *Proc. ODP, Init. Repts.*, 125: College Station, TX (Ocean Drilling Program).
[2] Department of Geosciences, University of Tulsa, Tulsa, OK 74104.
[3] Hawaii Institute of Geophysics, 2525 Correa Road, Honolulu, HI 96822.

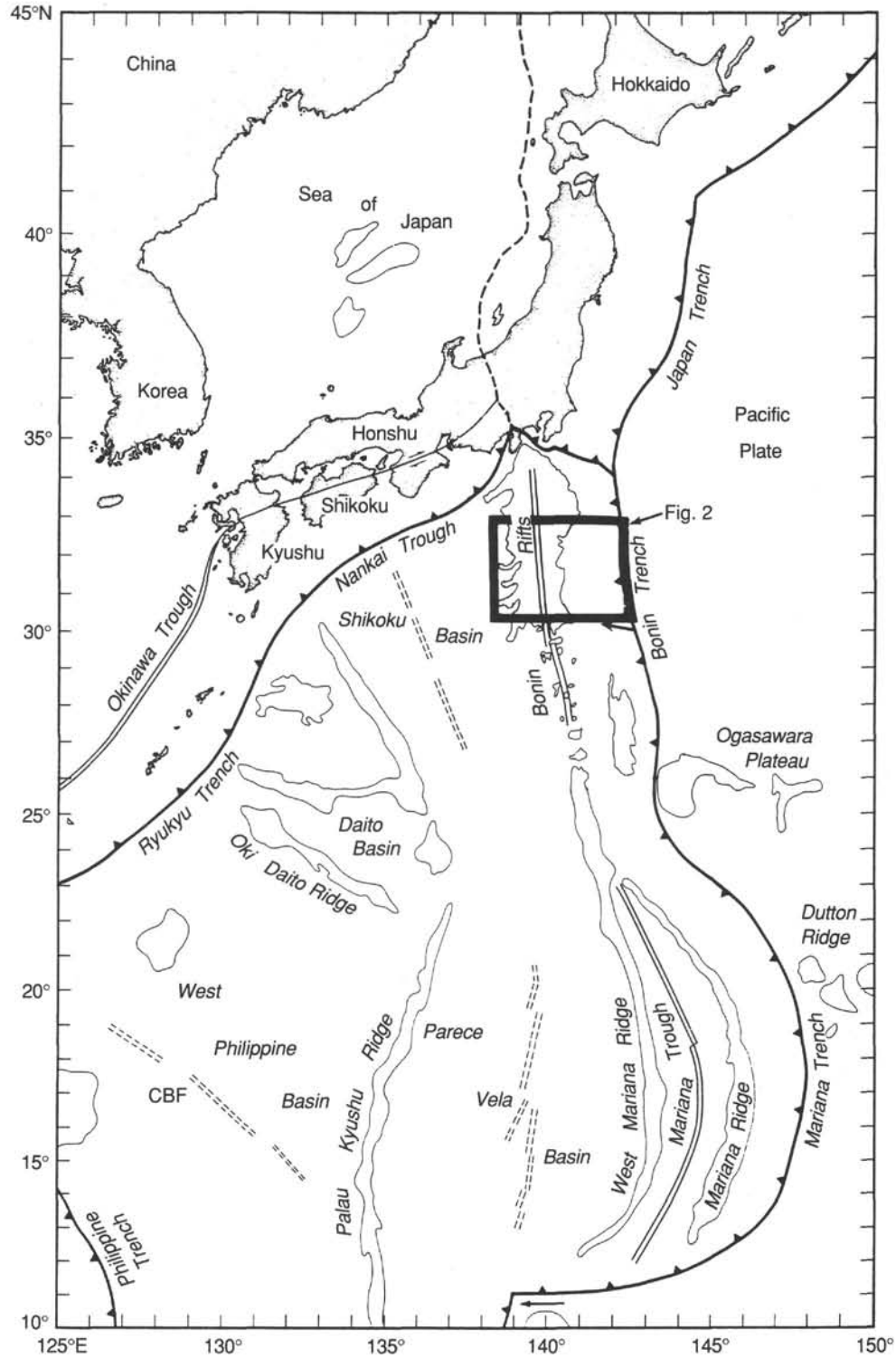

Figure 1. Regional map of the western Pacific Ocean showing the location of the survey area (Fig. 2) in the Izu-Bonin arc.

Seno and Maruyama, 1984). A bathymetric map of the survey area (Fig. 2) shows the locations of the seismic lines and gravity profiles discussed in the following sections.

A series of seamounts has formed along the inner trench slope between 20 and 50 km landward of the trench axis. These seamounts rise over 1 km above the surrounding seafloor, and some are up to 20 km in diameter. Small sedimentary basins have formed arcward and between several of these seamounts. Chloritized mafic and serpentinized ultramafic rocks have been dredged from the flanks of several of these features (Ishii et al., in press; Maekawa et al., in press). Similar structures in the Mariana arc to the south are the result of the emplacement and protrusion of serpentinite diapirs (Fryer et al., 1985; Fryer and Fryer, 1987). However, the

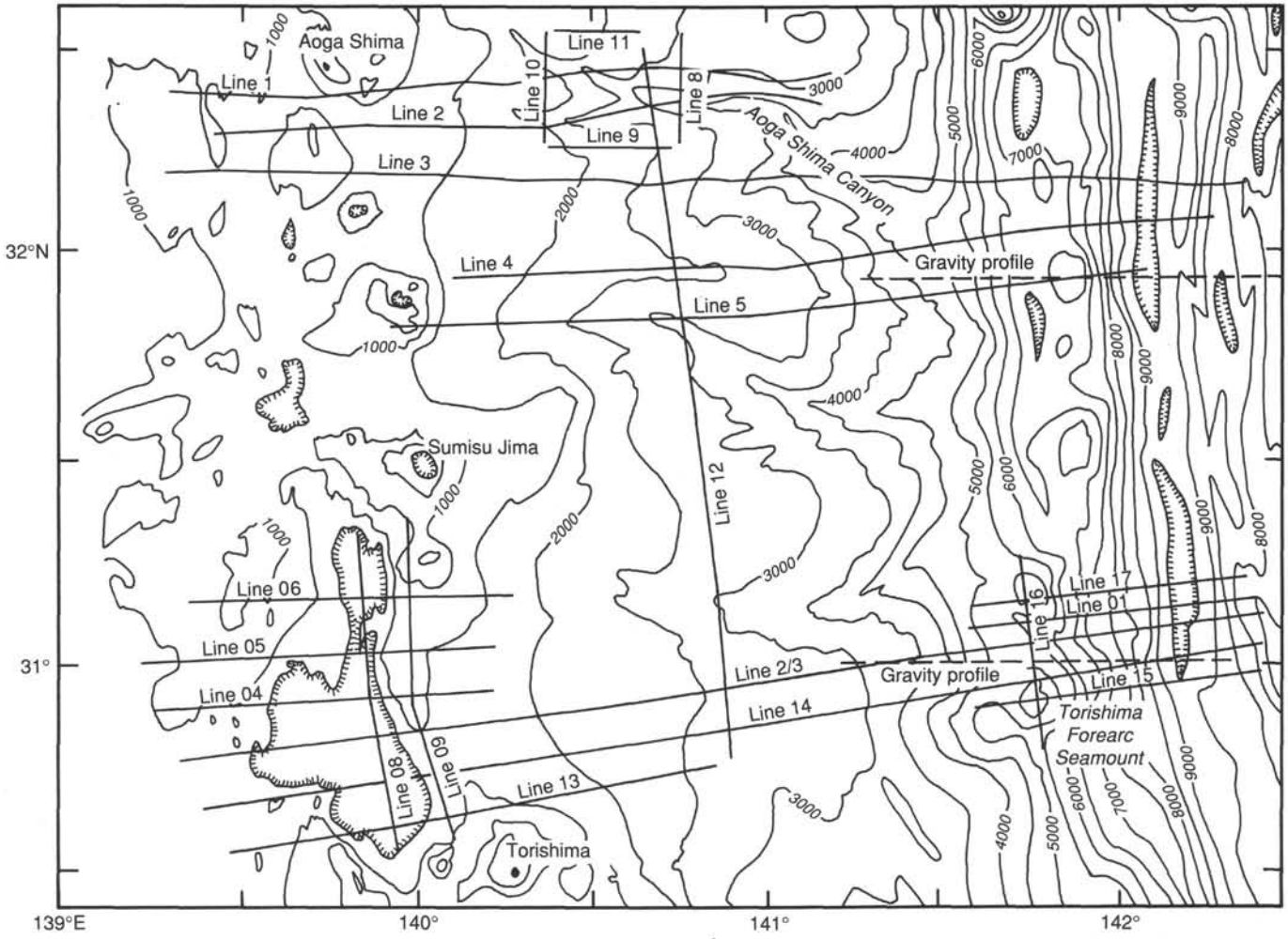

Figure 2. Bathymetry map of the survey area, modified after Taylor and Smoot (1984), showing the locations of our seismic lines (solid lines) and gravity profiles (dashed lines). The specific area of interest in this paper is east of 141.5°. Contour interval = 500 m.

Mariana forearc is highly fractured, providing conduits for the diapirs, whereas SeaMARC II side-scanning data indicate that the Izu-Bonin forearc is much less fractured. These observations led Fryer and Fryer (1987) to suggest that the entire Izu-Bonin outer forearc has undergone regional serpentinization and uplift and that discrete highs are caused by a locally greater degree of hydration and metamorphism. One of us (B. T.) therefore proposes that these seamounts were formed by localized protrusions of serpentinized material that moved up the décollement between the overriding forearc and the subducted plate. There are thus several possible explanations for these seamounts: simple diapirs, regional serpentinization, and/or deep-seated intrusions. In this chapter, we use seismic data to describe the structures within the seamounts and the shallow sedimentary features within a basin formed between two of the seamounts to illustrate their historical development. We will then examine information provided by gravity data and propose a model for seamount formation.

SEISMIC INTERPRETATION

The acquisition parameters for the seismic data are given in Table 1. The processing sequence in Table 2 is a standard processing sequence, except for the final step, depth conversion. Depth conversion velocity functions were obtained by integrating our stacking and migration velocities with available seismic-refraction velocities from this region (Hotta, 1970; Houtz et al., 1980). These velocities were further refined in the shallow section by comparison with logging velocities at Sites 783 and 784 ("Site 783" and "Site 784" chapters, this volume).

Table 1. Field parameters for the acquisition of seismic-reflection data.

Recording vessel	*Fred H. Moore*
Source	Bolt air-gun array (3065 in.^{3})
Streamer	96 channels
Group interval	33.3 m
Shot interval	30–60 m
Sample rate	2 ms
Recording format	SEG D (demultiplexed)

A detailed bathymetric map of the specific area of interest in this paper, which shows the locations of seismic lines, the position of a gravity profile by the Geologic Survey of Japan, and the location of ODP Sites 783 and 784, is given in Figure 3. There are two seamounts in the center of this region and one to the north. The southernmost seamount has been informally named Torishima Forearc Seamount by Ishii et al. (in press). A small sedimentary basin has formed west of and between the two central seamounts (Fig. 3). Seismic line 14 crosses part of this basin and the flank of a seamount and continues down into the trench axis, as shown in Figure 4.

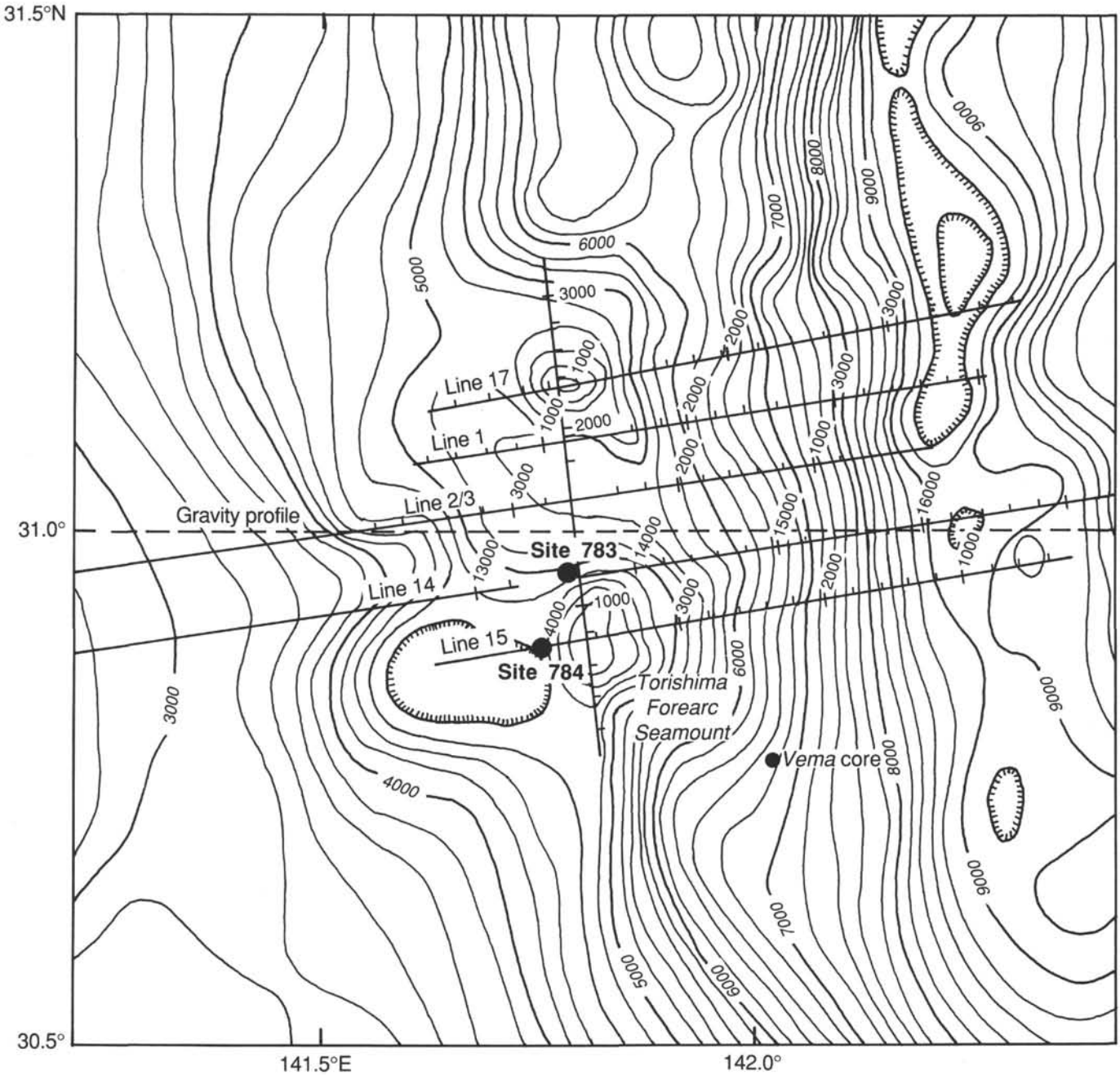

Figure 3. Detailed bathymetric map of the survey area showing the locations of our seismic lines and the gravity profile discussed in the text. Numbers along the lines correspond to the common-depth-point (CDP) numbers on the seismic sections. Bathymetry data from the Geologic Survey of Japan and the U.S. Navy. Contour interval = 200 m.

Note that sediments are scarce outside the basin.

The two central seamounts exhibit internal structures on all the seismic lines. Several internal reflections visible on line 15 (Fig. 5A) over Torishima Forearc Seamount are emphasized in the line drawing of the depth-converted section (Fig. 5B). Features dipping away from the center of the seamount on the time section become subhorizontal on the depth section because of the relatively high velocity (1.6–1.8 km/s) of the seamount material compared to the water velocity. All of these reflectors are fairly weak and discontinuous and exhibit dips ranging from 35° to the east to 20° to the west. However, they also show sufficient continuity on this line, and on the adjoining lines, to suggest that there are regionally significant seismic horizons between 1.2 and 2.5 km below seafloor. Between these deep horizons and the surface is a region containing few coherent reflectors that persists throughout the body of this seamount. Ishii et al. (in press) and Maekawa et al. (in press) dredged sheared serpentinites from the seafloor where this layer crops out, which they interpreted as having formed during the emplacement of a serpentinite diapir.

Figure 6 shows part of seismic line 16, a strike line crossing Torishima Forearc Seamount near its crest. The reflections that are visible within the seamount on line 15 also appear on this line. Although these reflections are more discontinuous than those on line 15, they can be traced to the north, where they are visible on line 14 (Fig. 7). The shallow region above

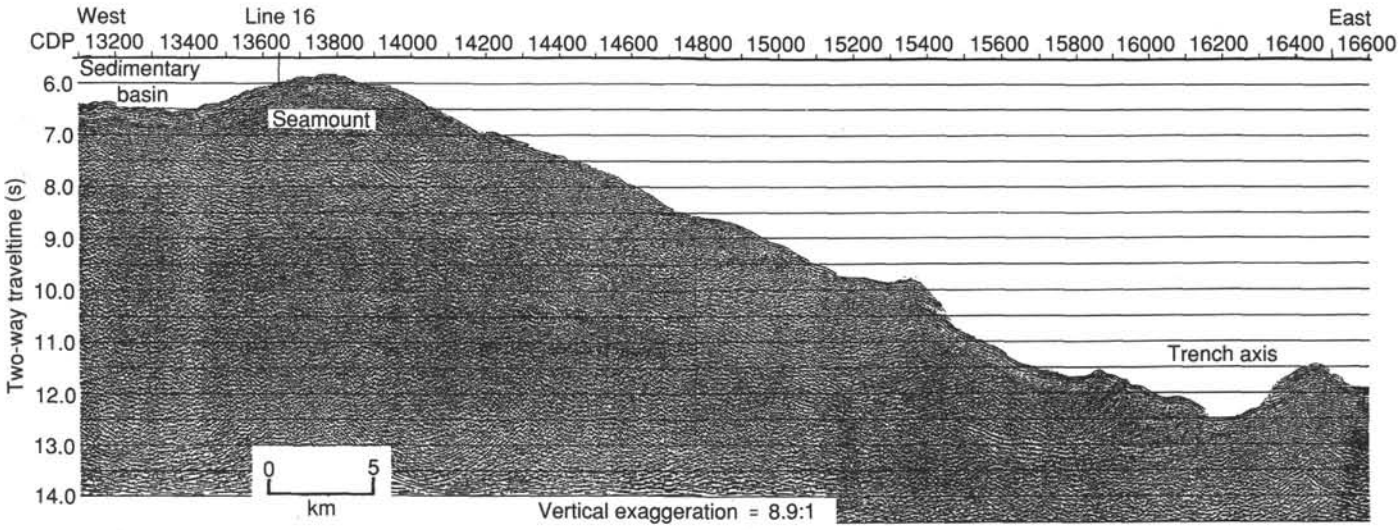

Figure 4. Time section of seismic line 14 from the trench to the seamount, with the location of the sedimentary basin and the seamount.

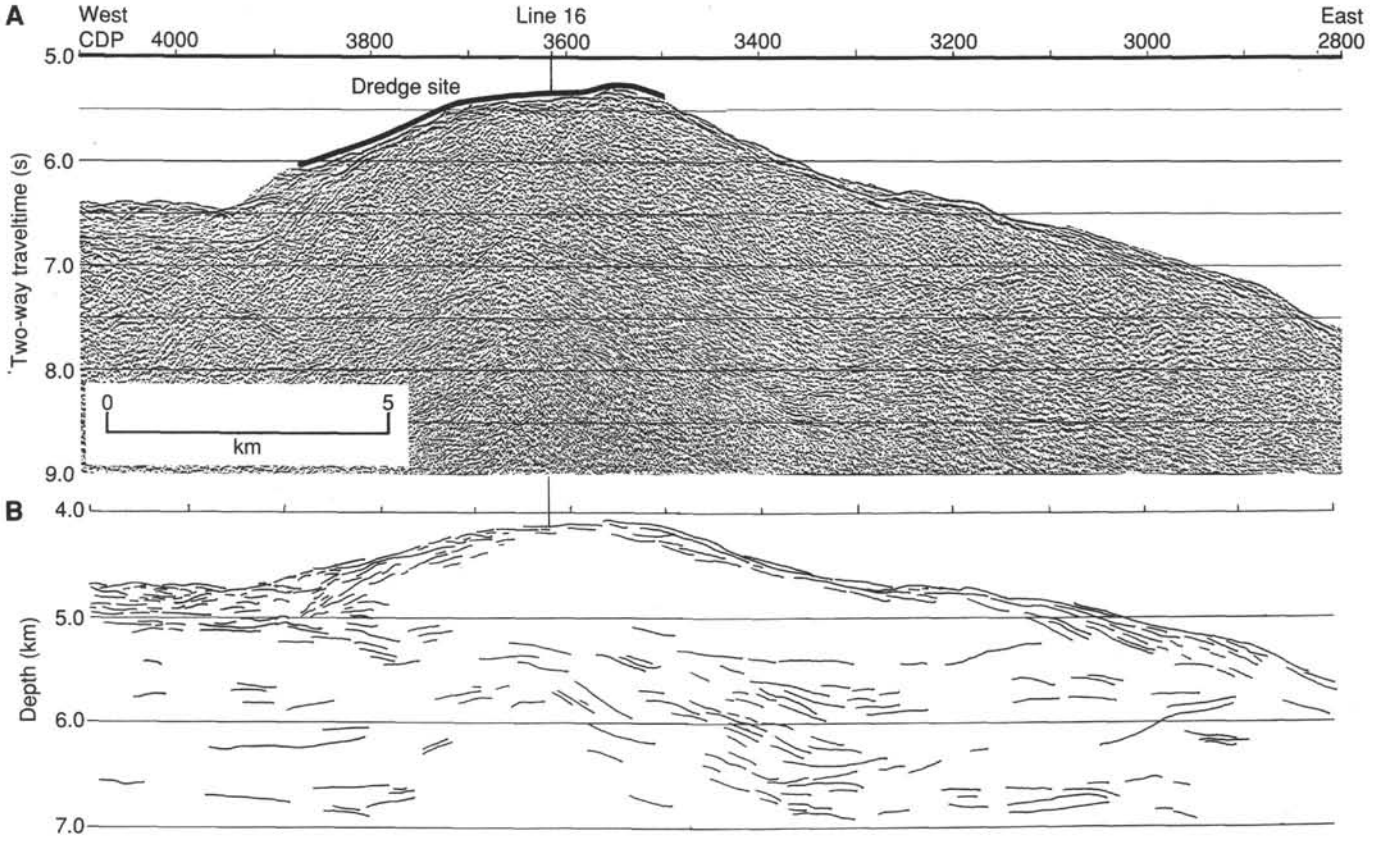

Figure 5. Seismic line 15. **A.** Time section showing a high-amplitude arrival between CDP 3000 and 3200 at 10-s depth, which appears to be sideswipe, uplifted sediments west of CDP 3800 at 6.2 s, and reflections within the seamount at 7.2 s from CDP 3200 to 3500. The dredge location is from Maekawa et al. (in press). **B.** Depth section emphasizing the internal structure of the seamount. The dipping reflectors at 6.0 s below CDP 3200 become subhorizontal on the depth section.

6.5 s between common-depth-points (CDP) 500 and 1100 contains few coherent reflectors and can be traced as far north as line 14.

Site 783 is near the intersection of lines 16 and 14 (Fig. 7). About 150 m of sediment overlies the seamount on the lower north flank, as seen on the depth sections of these lines. A reflector marking the upper limit of the material forming the seamount crops out several kilometers to the east, where serpentinite has been dredged (Maekawa et al., in press). This reflection may be the interface between the sediments and serpentinite forming the seamount, which was confirmed by drilling that encountered serpentine underlying sediments at 120 m below seafloor (mbsf) at Site 783 (see "Site 783" chapter). The shallowest internal reflector is observed on line 14 (Fig. 7) at about 420 mbsf (300 m below the sediment/serpentinite boundary). Based on reflection character, this

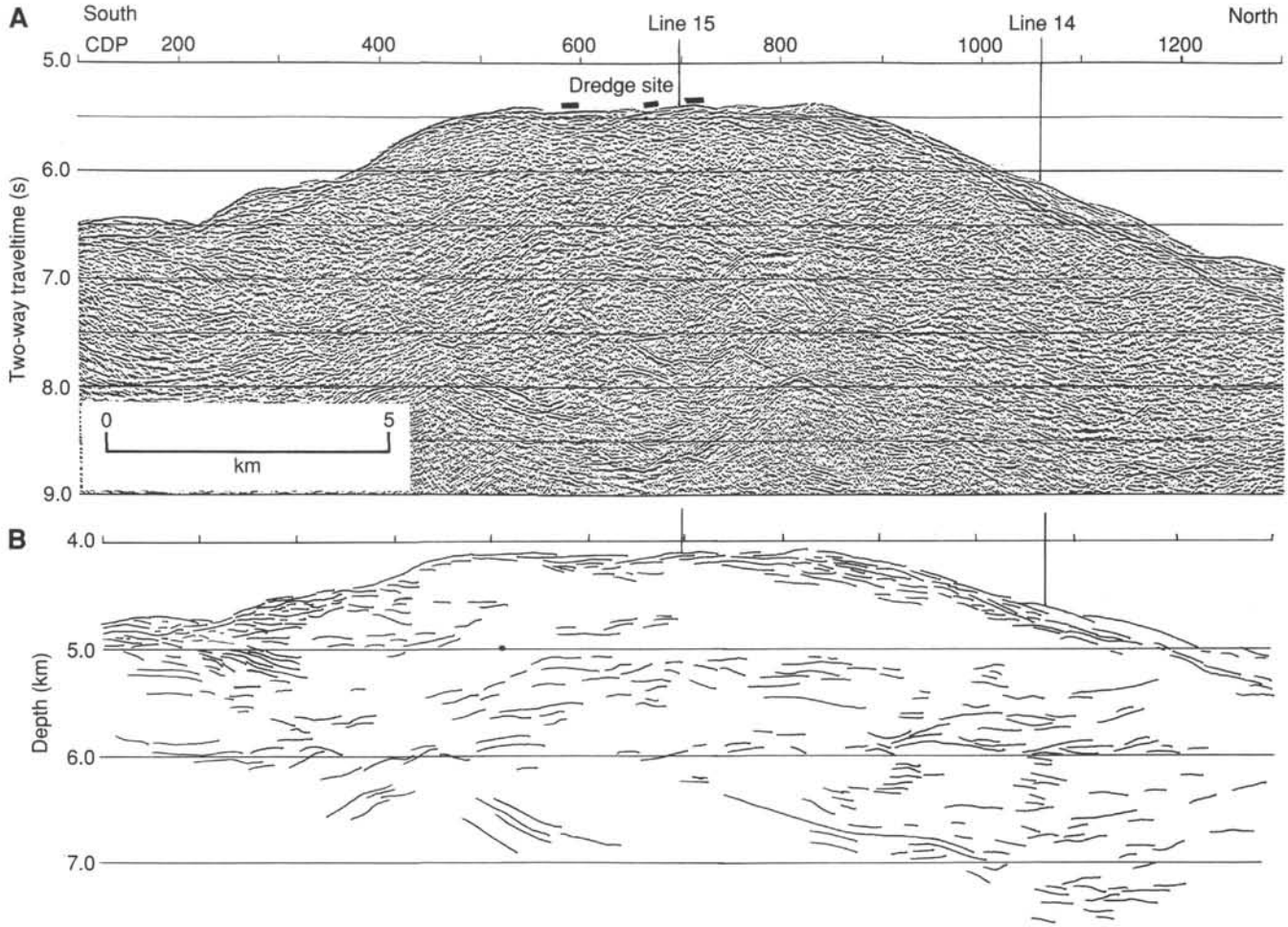

Figure 6. Seismic line 16. **A.** Time section of the part of the line crossing the seamount showing uplifted sediments on the north flank. The three dredge haul locations are from Maekawa et al. (in press). **B.** Depth section showing reflections within the seamount.

Table 2. Processing sequence for the seismic-reflection data.

Edit noisy traces	
Resample to 4 ms	
Sort to 16.67-m common-depth-point (CDP) bins	
Velocity analysis	
Normal moveout	
Mute	
Common-depth-point stack	
Predictive deconvolution	
60-ms prediction distance	
180-ms operator length	
720-ms design window	
Bandpass filter	
Water bottom to 500 ms below water bottom	10-15-50-60 Hz
500 to 1000 ms below water bottom	10-15-40-50 Hz
1000 ms below water bottom to end of record	6-10-35-45 Hz
Finite-difference migration	
Gain	
500 ms automatic gain control	
Depth conversion	

reflector appears to correlate with the reflector marking the base of the sediment farther west. This 420-m reflector may represent the original surface upon which the serpentinite flows forming the seamount were extruded. Unfortunately, drilling was unable to penetrate deep enough to test this interpretation.

Both seamounts are covered by a thin (0–200 m) veneer of sediment (Figs. 5–8). Lines 15 and 17 (Figs. 5 and 8, respectively) indicate that the sediment is commonly thicker on the flanks than on the summit of the seamounts, perhaps as a result of downslope transport. Both seamounts have an irregular surface topography, with maximum dips of 10°–17°. A piston core (*Vema* 21-077, from 30°49′N, 141°59′E, at a water depth of 6790 m; Fig. 3) on the east flank of Torishima Forearc Seamount recovered 4.2 m of gravelly serpentinite sand. This and the discontinuous, hummocky near-surface reflectors suggest that the seamounts themselves may be sediment sources, producing either primary serpentinite flows or secondary slump and debris-flow deposits. The basal sedimentary section at Site 784, drilled on the lower western flank of the southern seamount, contains a mixture of silt-sized serpentine derived from the seamount together with hemipelagic clays (see "Site 784' chapter).

Up to 900 m of strata has accumulated in basins to the west of and between the two seamounts (line 1: CDP 700–1300, 8.3 s; Fig. 9), in contrast to the generally less than 100 m of sediment covering the trench slope to the east and west (line 1: CDP 1800, 8.5 s). Drilling at Sites 783 and 784 (see the site chapters) showed that most of the seamount flank sediment consists of middle Miocene and younger hemipelagic vitric clays. The surrounding basins are probably filled with hemipelagic clays, together with sedimentary serpentinite derived

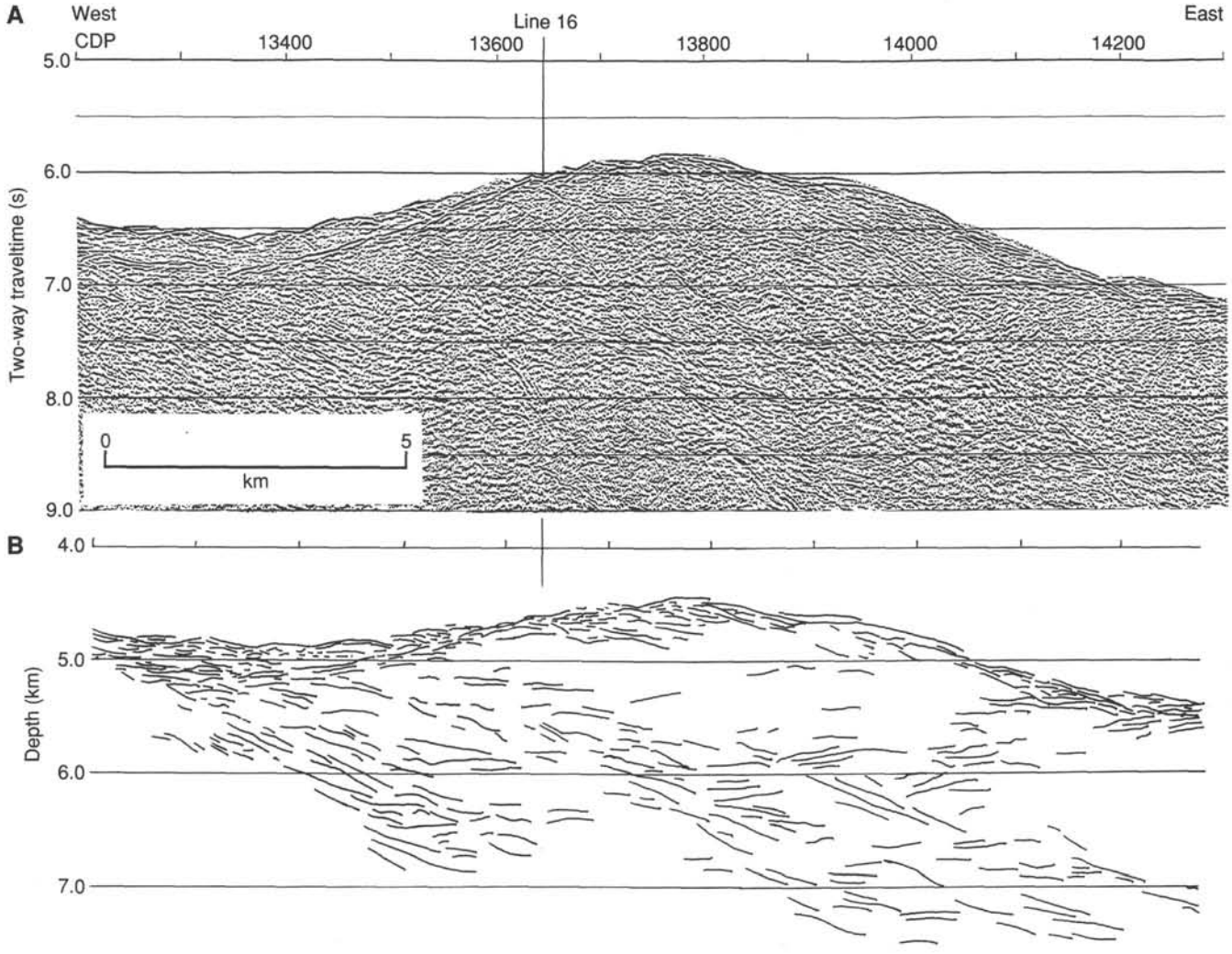

Figure 7. Seismic line 14. **A.** Time section showing disturbed, and possibly slumped, sediments on the west flank of the seamount. The reflector at 7.0 s between CDP 13400 and 13500 appears to be a continuation of the surface marking the bottom of the sediments to the west. **B.** Depth section showing eastward-dipping basement reflections.

from the seamounts, as well as some sediment transported from the volcanic arc to the west. The basins are partially bounded by spurs and ridges trending west-northwest and north-northeast from both seamounts, south-southwest from Torishima Forearc Seamount, and southeast from the northern seamount (see Fig. 3). Seismic line 17 (Fig. 8) along the ridge forming the northern limit of the central basin shows that the strata, which are 500 ms thick on line 1 (Fig. 9), pinch out to the north before reaching this line. The central basin drains to the east through a saddle between the seamounts; the sediment has overtopped the ridge formed by the coalesced spurs from both seamounts (see Fig. 10).

We define four seismic stratigraphic sequences in the basin between the seamounts, based on depositional patterns visible in the seismic data of Figures 9 through 11. Site 783, drilled on the north flank of the southern seamount, penetrated Quaternary to lower Pliocene vitric hemipelagic material above serpentinite basement. This section is the thin basin flank part of sequences 2 through 4. Sequence 1 rests unconformably on truncated, moderately to steeply dipping reflectors within basement (Fig. 11). This sequence is restricted to topographic lows, where it laps onto basement surface irregularities (e.g., line 16: CDP 1620, 8.25 s; Fig. 11). The internal character of sequence 1 is generally chaotic, but in some places exhibits parallel, though dipping, stratification (e.g., line 16: CDP 1600, 8.0 s; Fig. 11). On the flanks of the basin (line 16: CDP 1300–1600 and 1950–2100; Fig. 11), the internal stratification and upper and lower sequence boundaries dip toward the basin axis. We suggest that this sequence consists of serpentinite detritus shed from the adjacent serpentinite seamounts. Serpentinite detritus likely also forms at least a small percentage of the younger sequences.

Sequences 2 through 4 onlap older sequences along the northern side of the basin, onlap basement on the west side of the basin (lines 1 and 2/3; Figs. 9 and 10, respectively), and thin onto the southern flank (Fig. 11). On the east side of the basin, sequences 2 and 3 thin along the spur projecting from the northern seamount (line 1; Fig. 9). Sequence 4 also thins onto the flank of the southern seamount, but onlaps sequence 3 adjacent to the northern seamount. These sequences are thickest within the basin, and all exhibit parallel to hummocky stratification. Sequence 4 is mounded at the west side of the basin on line 1 (CDP 700–900; Fig. 9). Sequences 2, 3, and 4 consist of dominantly hemipelagic sediment underlying the flanks of the seamounts. These sequences should contain significant percentages of hemipelagic sediment, but also represent turbidites generated from slumping of hemipelagic material from the flanks of the seamounts. Detritus carried

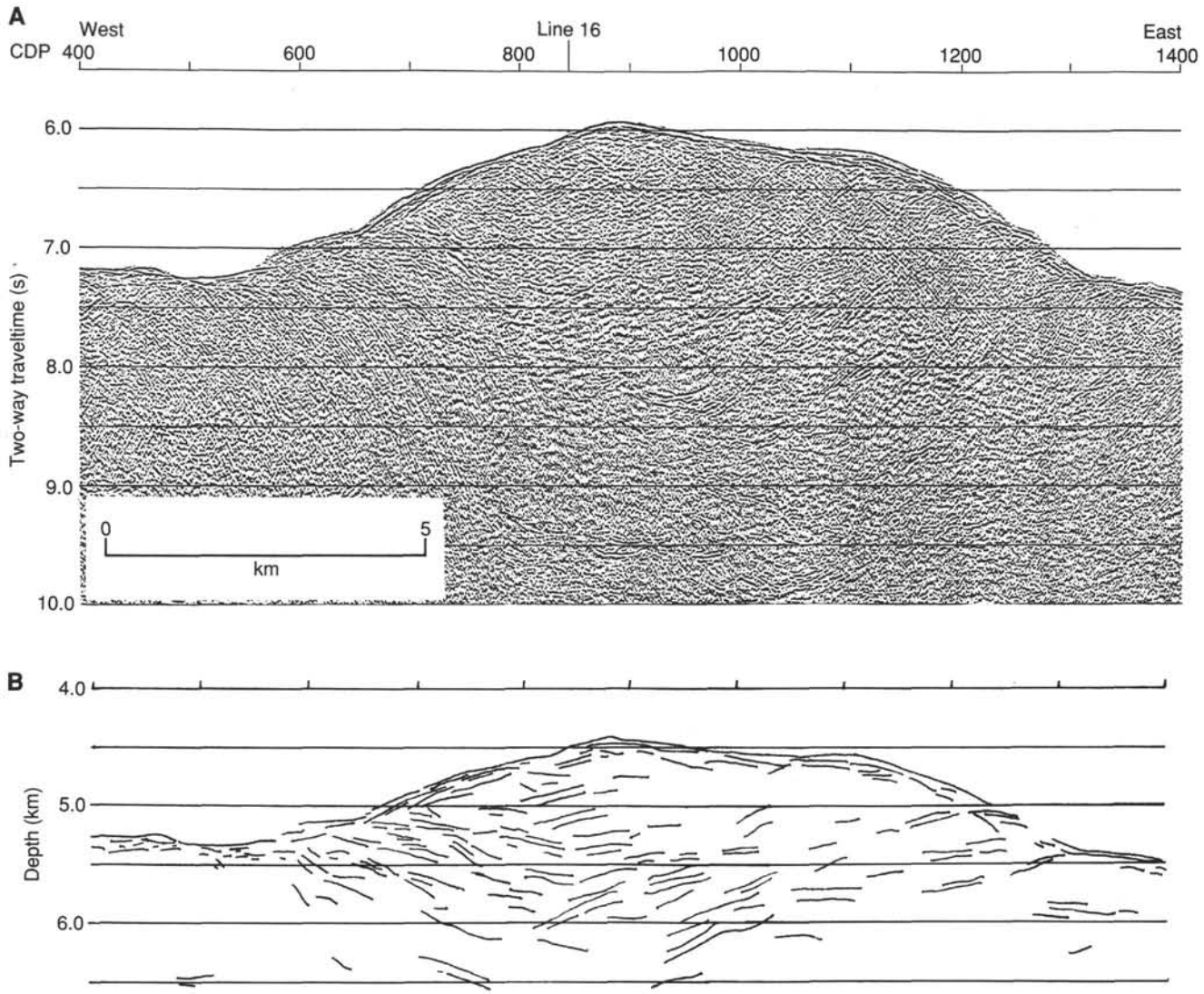

Figure 8. Seismic line 17. **A.** Time section showing very few sediments west of the seamount. **B.** Depth section showing the internal reflection of the seamount.

from the volcanic arc is probably a minor component of these turbidites, as indicated by the drilling at Sites 783 and 784 (see site chapters). Much erosion and redeposition of these sequences probably has occurred, as indicated by the internal mounding and lack of continuity (line 16: CDP 1900–2100; Fig. 11). Small, near-surface channels occur on line 2/3 (CDP 2500–3200; Fig. 10), and evidence of erosional truncation is widespread (e.g., line 2/3: CDP 2400–2600; Fig. 10) and occurs as far north as line 5 (CDP 10400–10600; Fig. 12).

Seismic line 5 (Fig. 12) shows a similar set of sequences almost 90 km to the north (Fig. 2). The sequences visible on this line may not be directly correlative to those discussed previously because they were influenced by sediments transported down Aoga Shima Canyon (Fig. 2). However, these northern sequences do show similar patterns of thinning toward the seamount (CDP 11200, 8.3 s; Fig. 12), suggesting that similar tectonic forces have been acting on this part of the forearc.

The history of seamount diapirism is recorded in the basin fill. Initial formation of the seamounts and protrusion of serpentinite probably took place during the deposition of sequence 1. By the time of deposition of sequence 2, a morphologic basin had developed by formation of the seamounts. The seamounts then became a barrier to sediment transport down the trench slope, and younger sequences were ponded in the basin. Relative uplift of the seamounts was episodic during deposition of sequences 2, 3, and 4. Sequence 2 onlaps both the north and south seamounts, but is now tilted toward the basin on the flanks of both seamounts, indicating relative uplift of both seamounts. Sequences 3 and 4 onlap the flanks of both seamounts, but are tilted toward the basin only on the flank of the southern seamount. This suggests that the southern seamount was actively deforming during the deposition of both sequences, while the northern seamount was quiet. Continuing activity at the southern seamount is indicated by erosional truncation of recent deposits on its flanks (e.g., line 16: CDP 1400–1500; Fig. 11) and a basinward tilting of the seafloor at this same location.

GRAVITY INTERPRETATION

We constructed a two-dimensional model along a gravity profile collected by the Geologic Survey of Japan at 31°N (Figs. 3 and 13). In this model, the seafloor and the structures within 3 km of the seafloor were determined from the seismic-

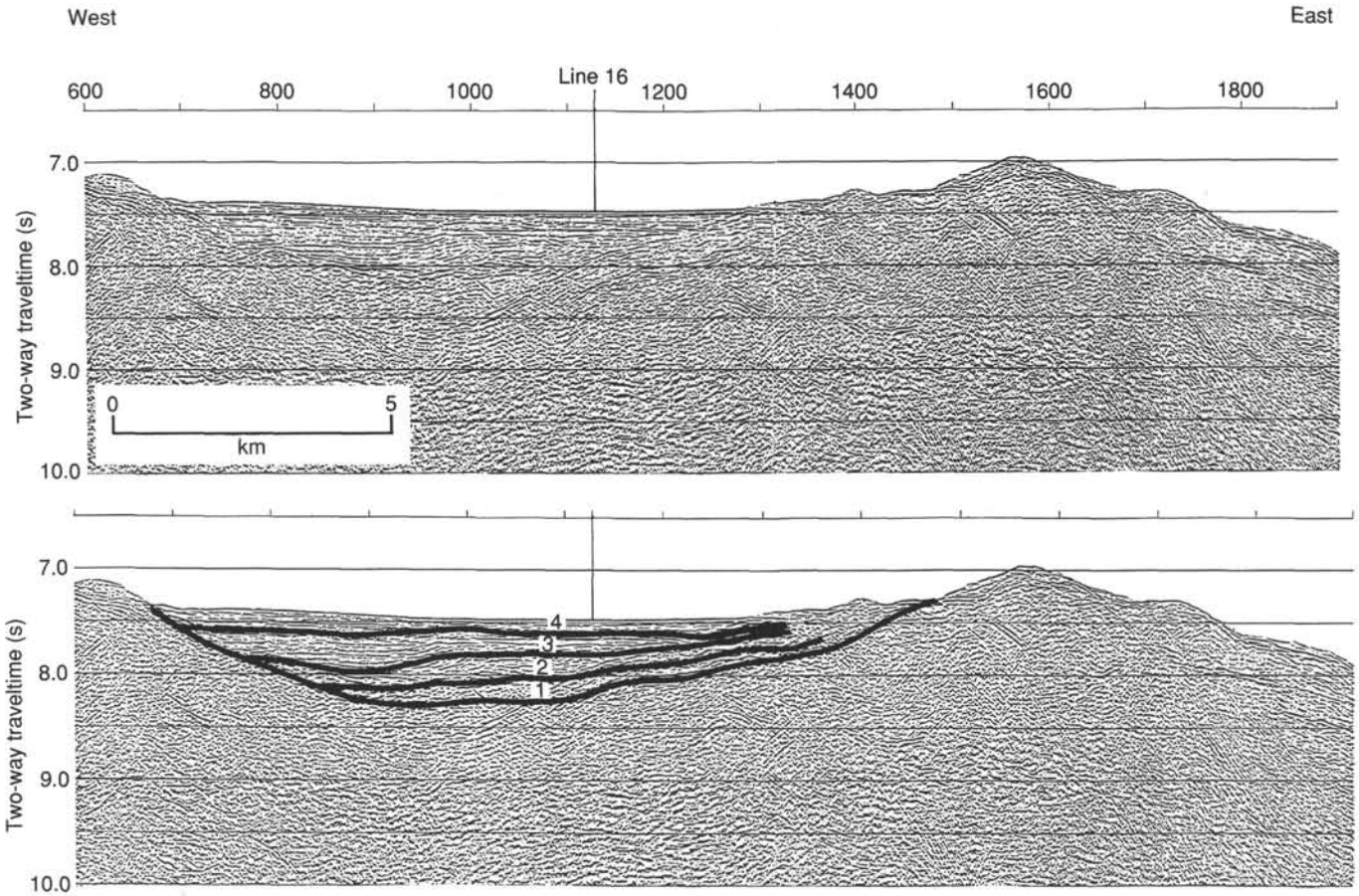

Figure 9. Time section of seismic line 1 showing sediments ponded behind a ridge protruding from the northern seamount. The numbered horizons in the seismic stratigraphic interpretation correspond to sequences 1–4.

reflection data of lines 14 and 2/3 (Figs. 4 and 10). The position of the subducting slab was constrained by refraction data (Hotta, 1970; Houtz et al., 1980) and earthquake seismology (Katsumata and Sykes, 1969; Roeker, 1985), so that the effects of the slab on the regional gravity trend were also incorporated. The crustal thickness beneath the forearc was approximated by refraction data, although there is some uncertainty in this region. Hotta (1970) placed the Moho at a depth of 20 km beneath the seamounts, whereas Houtz et al. (1980) placed it at 16 km just east of the seamounts. The thickness of the oceanic slab was constrained by refraction data and by modeling of the flexure of the subducting plate (Watts et al., 1980). Our initial model produced a reasonable fit to the observed data and provides some information about the deep structure in the vicinity of the basin (Fig. 13). No attempt was made to match the model and data at the western end of the profile, which crosses the eastern edge of the 2- to 4-km-thick forearc sedimentary basin. In the rest of this area, the observed and calculated fields match to within the noise level of the data (about 3 mGal) using only the bathymetry and a thin veneer of sediment filling the forearc basin. This indicates that any structures beneath the basin must have a low density contrast.

A second gravity profile at 32°N (Fig. 2) was also modeled (Fig. 14A). Seismic-reflection line 5 (Fig. 12) coincides with this profile, which crosses a seamount along the same trend as the seamounts at 31°N. B. T. (unpubl. data) has dredged serpentinized ultramafic and chloritized mafic rocks from this seamount. Figure 12 shows that this seamount is similar to those discussed previously in that it also has internal reflectors, except that this seamount has ponded a larger sedimentary basin behind it. A significant difference between this and the previous gravity model is that the bathymetric expression of the seamount produces a gravity high on the computed curve that is not present in the observed data (Fig. 14A). The difference between the computed and observed values is about 30 mGal. Matching of the observed gravity data required that a body be added to the model with a significantly lower density. A first approximation to such a body is shown in Figure 14B. A density characteristic of serpentinite (Coleman, 1971), 2.46 g/cm^3, was assigned to the seamount and the depth to the bottom of the serpentinized region was increased until a satisfactory fit to the observed data was obtained. The close match between the observed and calculated fields in Figure 14B indicates that beneath this seamount most of the forearc above the décollement is of low density, which suggests that it has undergone extensive serpentinization. In Figure 14A, the wavelength of the computed anomaly is approximately equal to the diameter of the seamount. If this holds true for the southern seamounts, the gravity profile at 31°N (Fig. 13) would have detected only the extreme edges of the anomalies caused by those seamounts. Because the profile at 31°N is off the flanks of the seamounts in this area it need not show any anomaly caused by the seamounts.

DISCUSSION AND CONCLUSIONS

Patterns of onlap and uplift of sediment in the Izu-Bonin outer forearc indicate that two midslope seamounts have been growing episodically during formation of a flanking basin, with Torishima Forearc Seamount experiencing more recent uplift

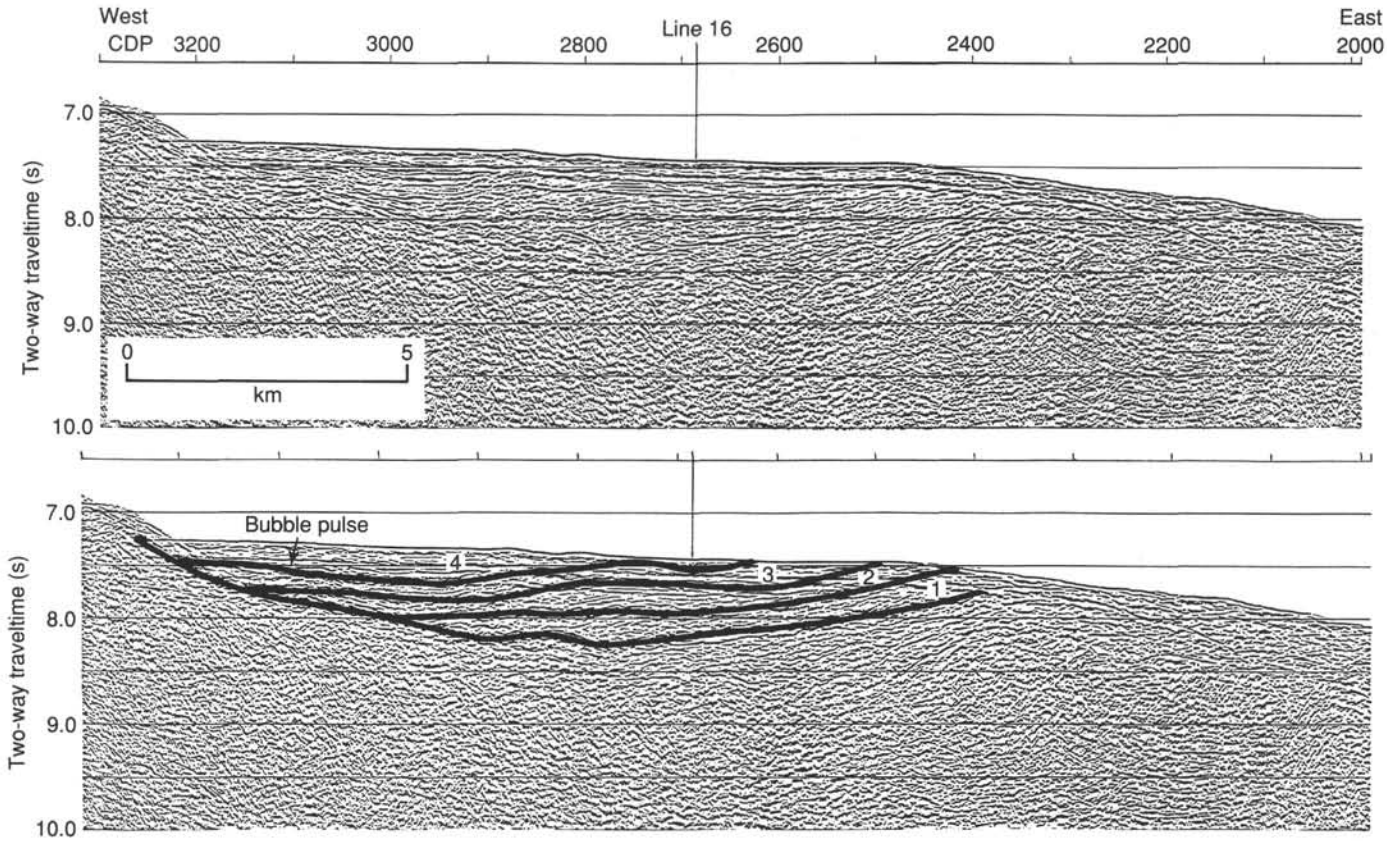

Figure 10. Time section of seismic line 2/3 showing sediments partially ponded behind a basement high. The numbered horizons in the seismic stratigraphic interpretation correspond to sequences 1–4.

(line 16: CDP 1200–1600; Fig. 11). Shallow regions within each seamount exhibit few coherent reflectors, as seen on lines 14, 15, 16, and 17 (Figs. 5–8), and may be composed of serpentinite flows. The deeper and seismically reflective regions beneath the seamount may be the original substrate onto which the serpentinite protruded.

Gravity modeling suggests that the seamounts are made up of low-density material and that the intervening sedimentary basins do not rest on a low-density substrate, so that the low-density (serpentinized?) zones must be limited to the seamounts. One possible model for the evolution of these forearc seamounts involves a two-stage process of emplacement and protrusion of small serpentinite diapirs, followed by uplift as a result of continued intrusion and serpentinization around the original conduits. Mass wasting of the seamounts, as well as primary serpentinite flows, could have deposited sequence 1 in the surrounding forearc basins. This stage ended by middle Miocene time, as evidenced by drilling at Site 784 ('Site 784' chapter).

The second stage in our model of seamount evolution involves intrusion of sills into the serpentinite edifice and serpentinization of the forearc around the original conduits. These processes resulted in the inflation of the seamounts and tilting of strata on their flanks. Serpentinization can increase volume by up to 40% (Thompson, 1960), which is adequate to explain the observed uplift. The serpentinization was centered on the original conduits and did not include the entire forearc, as indicated by the gravity modeling, which shows the low-density material confined to the seamounts. Tilting of the strata of sequences 2 through 4 indicates that this process may still be occurring in the southern seamount.

ACKNOWLEDGMENTS

This work was supported by NSF grant numbers OCE86-14687, OCE87-00826, and OCE89-96141. The authors would like to thank Bryan Tapp, William Underwood, Jamie Austin, and Mike Marlow for their review and critical comments of this paper and Mary MacKay, Todd Jimeson, and Robert Heaton for their help in processing the seismic data. Hawaii Institute of Geophysics contribution no. 2191.

REFERENCES

Aoki, Y., Tamano, T., and Kato, S., 1982. Detailed structure of the Nankai Trough from migration seismic sections. *In* Watkins, J. S., and Drake, C. L. (Eds.), *Continental Margin Geology*. AAPG Mem., 34:309–322.

Bloomer, S. H., 1983. Distribution and origin of igneous rocks from the landward slopes of the Mariana Trench: implications for its structure and evolution. *J. Geophys. Res.*, 88:7411–7428.

Coleman, R. G., 1971. Petrologic and geophysical nature of serpentinites. *Geol. Soc. Am. Bull.*, 82:897–918.

Crawford, A., Beccaluva, L., and Serri, G., 1981. Tectonomagmatic evolution of the Philippine-Mariana region and the origin of boninites. *Earth Planet. Sci. Lett.*, 54:346–356.

Fryer, P., Ambos, E. L., and Hussong, D. M., 1984. Origin and emplacement of serpentine diapirs in the Mariana fore-arc. *EOS, Trans. Am. Geophys. Union*, 65:1104. (Abstract)

_____, 1985. Origin and emplacement of Mariana forearc seamounts. *Geology*, 13:744–777.

Fryer, P., and Fryer, G., 1987. Origins of nonvolcanic seamounts in a forearc environment. *In* Keating, B. H., Fryer, P., Batiza, R., and Boehlert, G. W. (Eds.), *Seamounts, Islands, and Atolls*. Am. Geophys. Union, Geophys. Monogr. Ser., 43:50–63.

Honza, E., and Tamaki, K., 1985. The Bonin arc. *In* Nairn, A.E.M., and Uyeda, S. (Eds.), *The Pacific Ocean*: New York (Plenum Press), 459–502.

Horine, R. L., Moore, G. F., Taylor, B. T., and MacKay, M. E., 1988. Structure of the Bonin arc lower slope. *EOS, Trans. Am. Geophys. Union*, 69:1014.

Hotta, H., 1970. A crustal section across the Izu-Ogasawara arc and trench. *J. Phys. Earth*, 18:125–141.

Houtz, R., Windisch, C., and Murauchi, S., 1980. Changes in the crust and upper mantle near the Japan-Bonin Trench. *J. Geophys. Res.*, 85:267.

Hussong, D. M., and Uyeda, S., 1982. Tectonic processes and the history of the Mariana arc—a synthesis from the results of DSDP Leg 60. *In* Hussong, D. M., Uyeda, S., et al., *Init. Repts. DSDP*, 60: Washington (U.S. Govt. Printing Office), 909–929.

Ishii, T., Ozawa, H., Maekawa, H., Naha, J., Robinson, P. T., Kobayashi, K., and Uyeda, S., in press. Refractory peridotites from serpentinite diapiric seamounts in the Izu-Ogasawara-Mariana forearc. *Earth Planet. Sci. Lett.*

Katsumata, M., and Sykes, L., 1969. Seismicity and tectonics of the western Pacific: Izu-Mariana-Caroline and Ryukyu-Taiwan regions. *J. Geophys. Res.*, 74:5923.

Kodama, K., Keating, B., and Helsley, C., 1983. Paleomagnetism of the Bonin Islands and its tectonic significance. *Tectonophysics*, 95:25–42.

Maekawa, H., Shozui, M., Ishii, T., and Ozawa, H., in press. Ophiolitic seamounts in the Izu-Ogasawara forearc—evidence of serpentinite diapir. *Earth Planet. Sci. Lett.*

Roeker, S. W., 1985. Velocity structure in the Izu-Bonin seismic zone and the depth of the olivine-spinel phase transition in the slab. *J. Geophys. Res.*, 90:7771–7794.

Sakai, R., Kusakabe, M., Noto, M., and Ishii, T., in press. Origin of waters responsible for serpentinization of the Izu-Ogasawara-Mariana forearc seamounts in view of hydrogen and oxygen isotope ratios. *Earth Planet. Sci. Lett.*

Seno, T., and Maruyama, S., 1984. Paleogeographic reconstruction and origin of the Philippine Sea. *Tectonophysics*, 102:53–84.

Seno, T., Moriyama, T., and Stein, S., 1987. Redetermination of Philippine Sea plate motion. *EOS, Trans. Am. Geophys. Union*, 68:1474. (Abstract)

Taylor, B., and Smoot, N. C., 1984. Morphology of Bonin fore-arc submarine canyons. *Geology*, 12:724–727.

Thompson, R. B., 1960. Serpentinisation accompanied by volume changes. *Pac. Geol.*, 3:167–174.

Watts, A. B., Bodine, J. H., and Ribe, N. M., 1980. Observations of flexure and the geological evolution of the Pacific Ocean basin. *Nature*, 283:532–536.

Westbrook, G. K., and Smith, M. J., 1983. Long décollements and mud volcanoes: evidence from the Barbados Ridge Complex for the role of high pore-fluid pressure in the development of an accretionary complex. *Geology*, 11:279–283.

Ms 125A-105

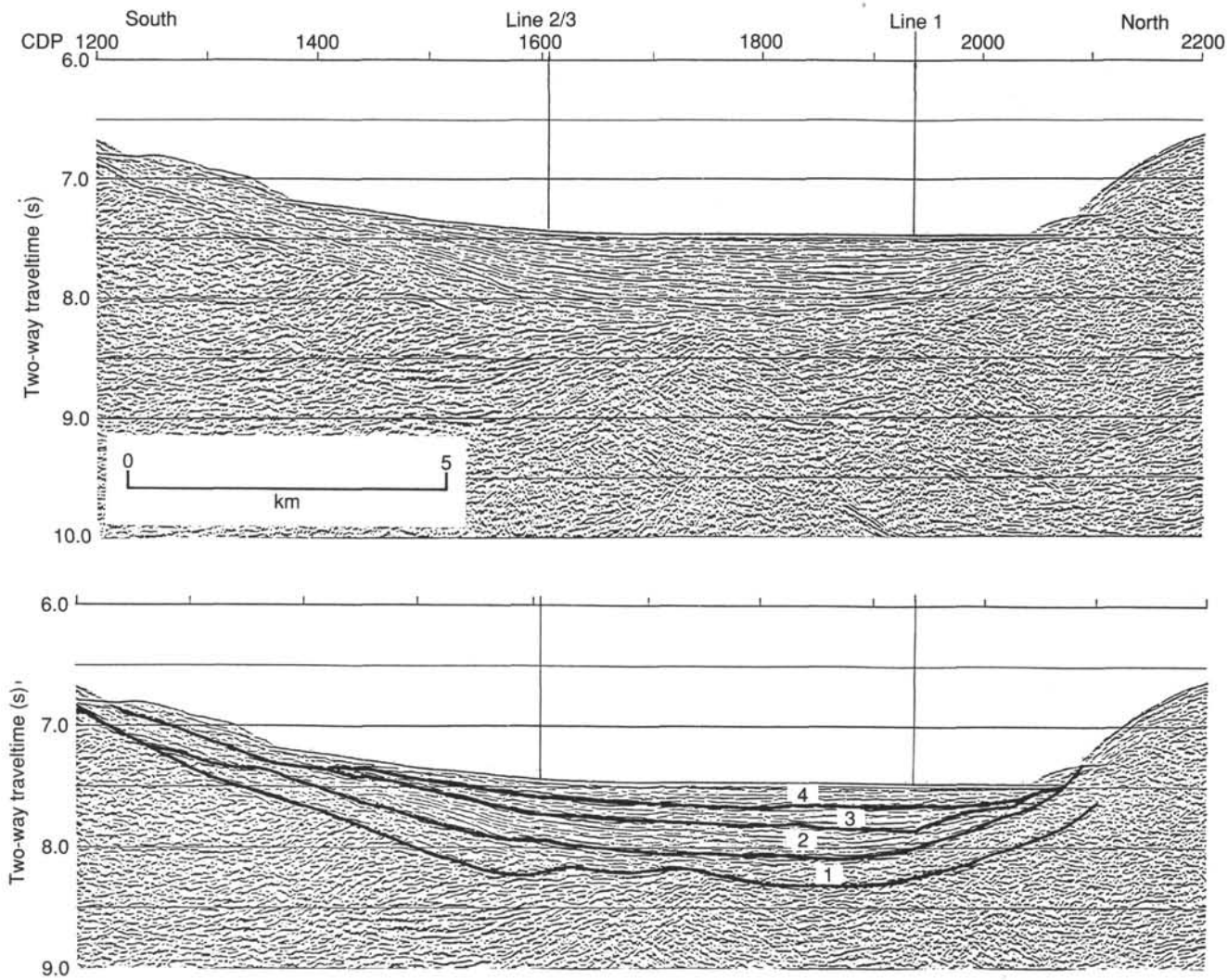

Figure 11. Time section of the basin part of seismic line 16. The numbered horizons in the seismic stratigraphic interpretation correspond to sequences 1–4.

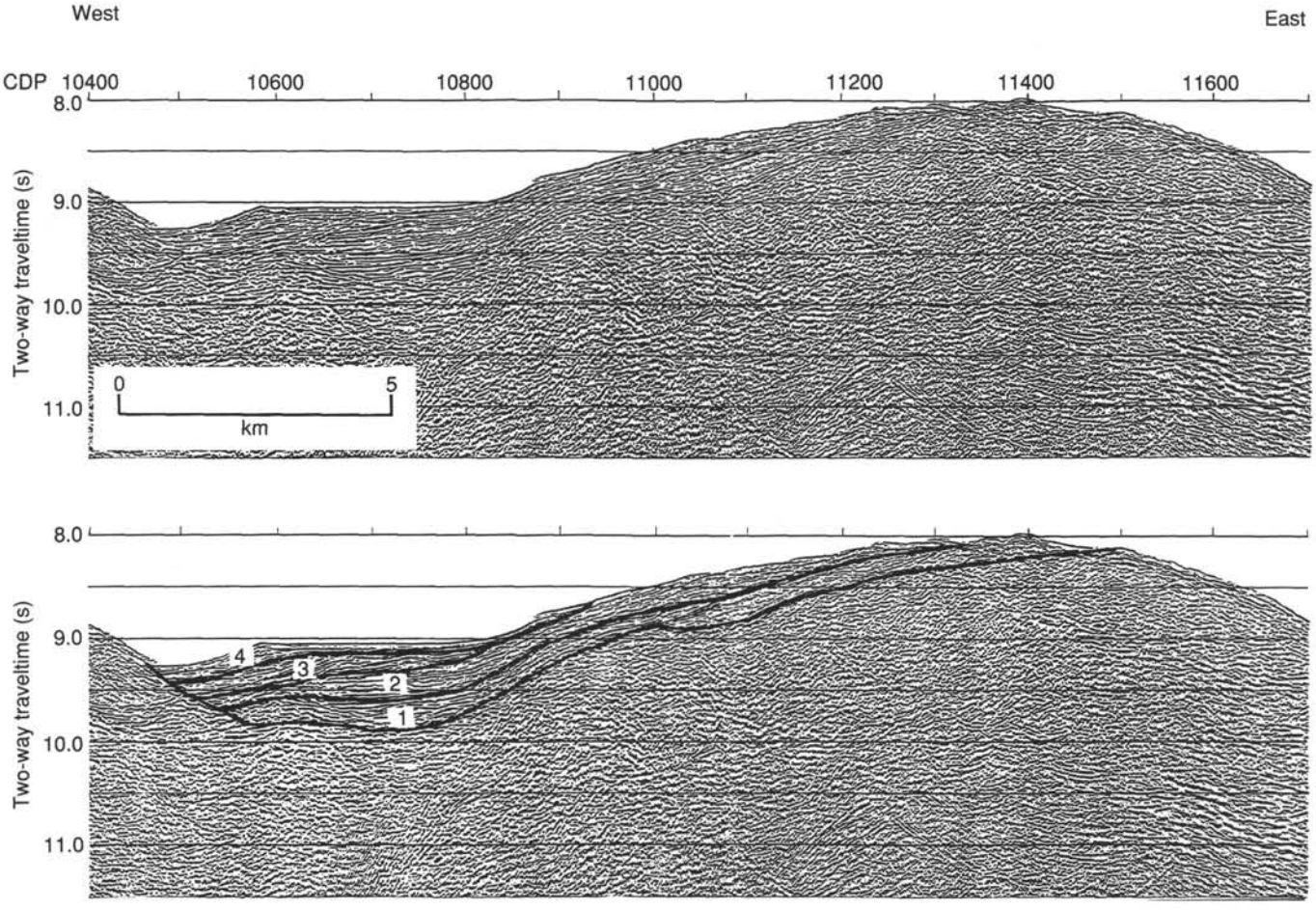

Figure 12. Time section of seismic line 5 at 32°N showing the seamount and sediments deposited in the basin to the west. The numbered horizons in the seismic stratigraphic interpretation correspond to northern area sequences.

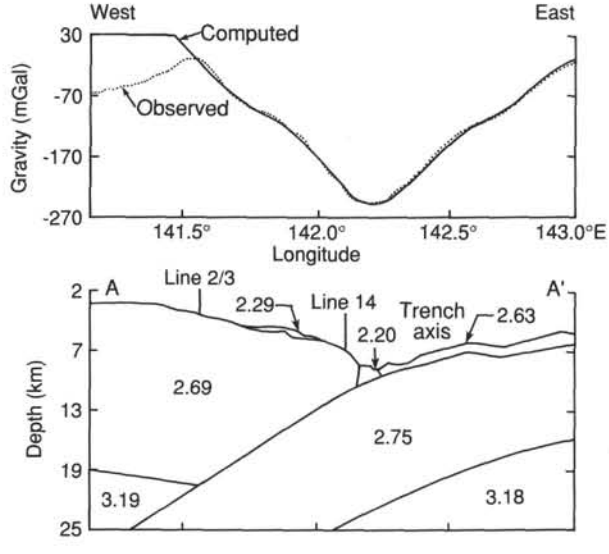

Figure 13. Gravity model along 31°N showing the subducting oceanic plate and trench-fill sediments. The dotted curve is the observed field; the solid curve is the calculated field.

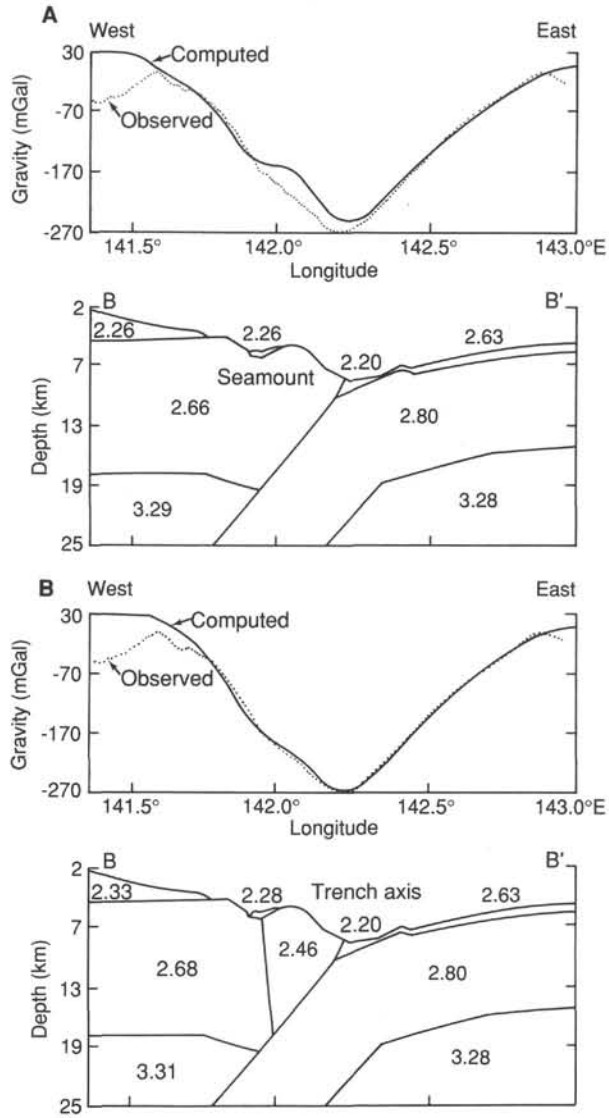

Figure 14. Gravity models along 32°N. The dotted curve is the observed field; the solid curve is the calculated field. **A.** A 30-mGal mismatch between the observed and computed fields in the vicinity of the seamount. **B.** A model with the seamount given a density characteristic of serpentinite has a significantly improved fit at 142°E.